HiSST: 2nd International Conference on
High-Speed Vehicle Science Technology
11–15 September 2022, Bruges, Belgium

# Bow Shock Instability Issues related to the Carbuncle Phenomenon

*Khalid A. Juhany*, Mahmood Khalid and Amjad Ali Pasha*

*Aerospace Engineering Department, King Abdulaziz University, Jeddah 21589, Saudi Arabia*
**Corresponding author: aapasha@kau.edu.sa*

## Abstract

During a heat transfer study past blunt axisymmetric bodies and other tangent-cone and Gasjet models equipped with forwarding flow facilities, the cylindrical shock exhibited atypical instability toward complete and comprehensive numerical resolution. Such undesired flow behavior is not present in real-life flows when such blunt axisymmetric models are launched in the atmosphere or tested in wind tunnels. The well-behaved shock in real life is observed as soon as the high Mach number flow impacts the model. The region before and immediately after the shock is fraught with high and low Mach numbers and extreme pressure conditions with invariable onset of disturbances traveling normal to the shock. It is suspected that such complex physical changes in a small region give rise to numerical errors that tend to compound in time and lead to shock instabilities, particularly close to the axis of symmetry. It had been postulated that various second and fourth-order fluxes provisioned to capture shocks in Euler flows may give rise to such instabilities, which it was reasoned would be removed through the use of viscous flows computed using the Navier Stokes equation. The present studies were conducted on a range of axisymmetric models. It was observed, however, that this carbuncle was most dominantly demonstrated on a Gasjet model, which effectively is a blunt, leading model with a sharply truncated front face.

## Introduction

The carbuncle instability was suspected to cause the numerical unsteadiness observed during a heat transfer study of various blunt axisymmetric bodies placed in hypersonic flow [1]. The computational convergence is noticeably faster when the flow immediately in front of a blunt axisymmetric nose, regardless of the bluntness values investigated, is allowed to proceed downstream smoothly as found past spherical-shaped noses. Fast and smooth convergence also occurred for flow past a blunt nose in front of a conical body with a backward-facing step for the tangent-slot film cooling model to alleviate heat during the hypersonic flight. In contrast, the convergence for the Gasjet model with a sharp truncated front face, as shown in Figure 1, was far more erratic and unwieldy. The solution would tend to converge, break down, and proceed towards convergence afresh. This behavior would repeatedly recapitulate without reaching a satisfactory permanent converged state. This computational phenomenon is well-known and well-versed in the aerodynamic CFD community. It is a numerical anomaly prevalent in regions fraught with muti-directional flows ranging from low subsonic to hypersonic Mach numbers, where the flow does not get a chance to resolve itself numerically in a confined space and time.

Roe et al. [2] have proposed the root cause of the carbuncle problem as an evolutionary process involving 'pimples', 'bleeding', which finally result in carbuncle. The "pimples" usually appear as triggering instability in close proximity to the shock, which then propagates downstream as alternately high and low-velocity layers. Once the threshold growth is reached, the low velocities develop regions of reversed flow that break out ahead of the shock to form the "carbuncle ."Chauvat et al. [3] observed that upwind schemes that preserved exact discontinuities, including the one used in the present computations, were beneficial for viscous flows but are prone to inviting carbuncle issues. Robinet et al. [4] examined the carbuncle problem by conducting the stability analysis of the continuous Euler

equations applied to a planar moving shock wave. The equation duly represents physical quantities in the unsteady flow:

$$q = \bar{q} + \hat{q}e^{i(k_x x + k_y y - \omega t)} \qquad (1)$$

Here $\bar{q}$ represents the mean quantity and $k_y$ is the wave number, whereas the complex portion of $k_x$ is the wave perturbation as the wave decays. The real part of ω is the perturbation frequency, while the imaginary part is the perturbation growth. The stability analysis showed an unstable mode that the normal mode form could not predict. Furthermore, there is a strong link between the theoretical form of the perturbation and the numerical behavior observed in the carbuncle phenomenon. Based on the above analysis, Mochetta et al. [5] further concluded that such CFD parameters as the CFL number, dissipative strategy, and order of accuracy demanded in a given computation contributed to the threshold above which the carbuncle is invoked. Kemm [6] emphasized numerical viscosity as a means of stabilizing the carbuncle and that shear viscosity was more dominant than the viscosity on entropy layers.

On the other hand, Rodionov [7] seeks the cure for carbuncle by experimenting with the Euler equations' solution by replacing the molecular viscosity coefficient with artificial viscosity. Kitimura et al. [8] have written a manuscript relevant to the present findings. As experienced in the current work, it was postulated that multidimensional anomalies were more likely to occur in three-dimensional flows than in two-dimensional problems. It was further argued that most dissipative measures used to correct one or two-dimensional carbuncles were not very useful for three-dimensional problems.

The current work includes a study of the carbuncle problem on a three-dimensional flat-faced truncated cone. It was understood from some of Kitimura et al. [8] discussions that the problem seems to disappear when the calculations are carried out on a 2D reflection plane model corresponding to the above 3D case. Towards this objective, the flow conditions applied to the 3D model were then applied to a 2D model to see if the carbuncle continued to persist in two- dimensions.

## CFD Studies

The present CFD studies evolved from the heat transfer work reported in [1]. The heat transfer studies were carried out with two cones of bluntness $\frac{R_N}{R_B}$ of about 0.1 and 0.3 models, a Gasjet model with a truncated flat nose, and a blunt spherical nose model with a tangent-slot film coolant located at the nose cone juncture. The models are detailed in reference [9], containing comprehensive experimental measurements used to verify the CFD work.

It was noted during the above CFD studies that the computations past flat nosed model suffered from carbuncle issues. A single slice of the mesh used in this study is shown in Figure 1. The 3D version was created by rotating this mesh in an azimuthal direction through 90 equivalent steps. The 2D representative calculations were carried out on this 2D mesh to demonstrate that the carbuncle problem plaguing the 3D flow computations was non-existent in 2D. The actual details of the three NASA models are provided in Ref. [9] and appropriately shown in Figure 2.

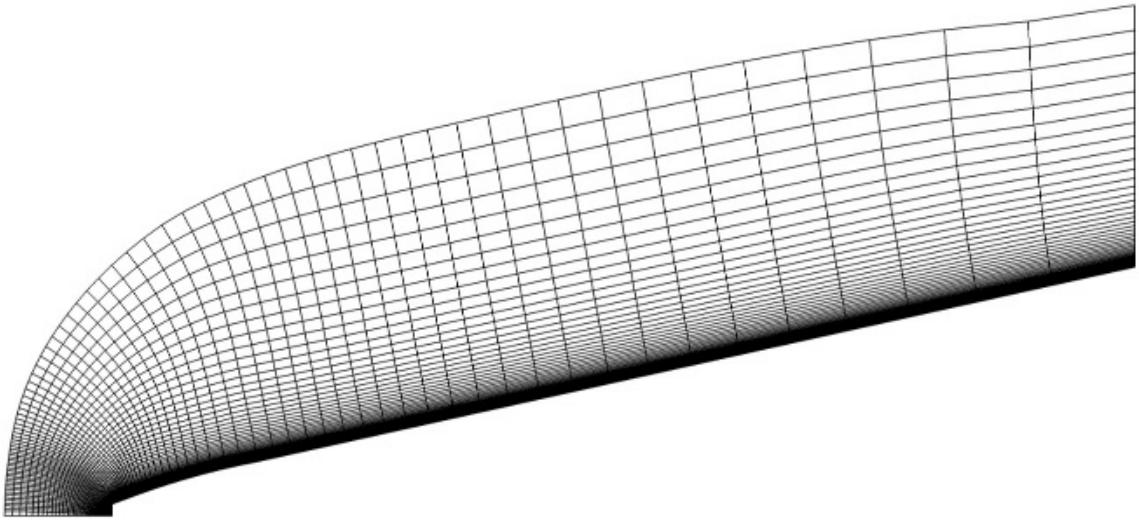

Figure 1. The 2D (75 X 120) mesh.

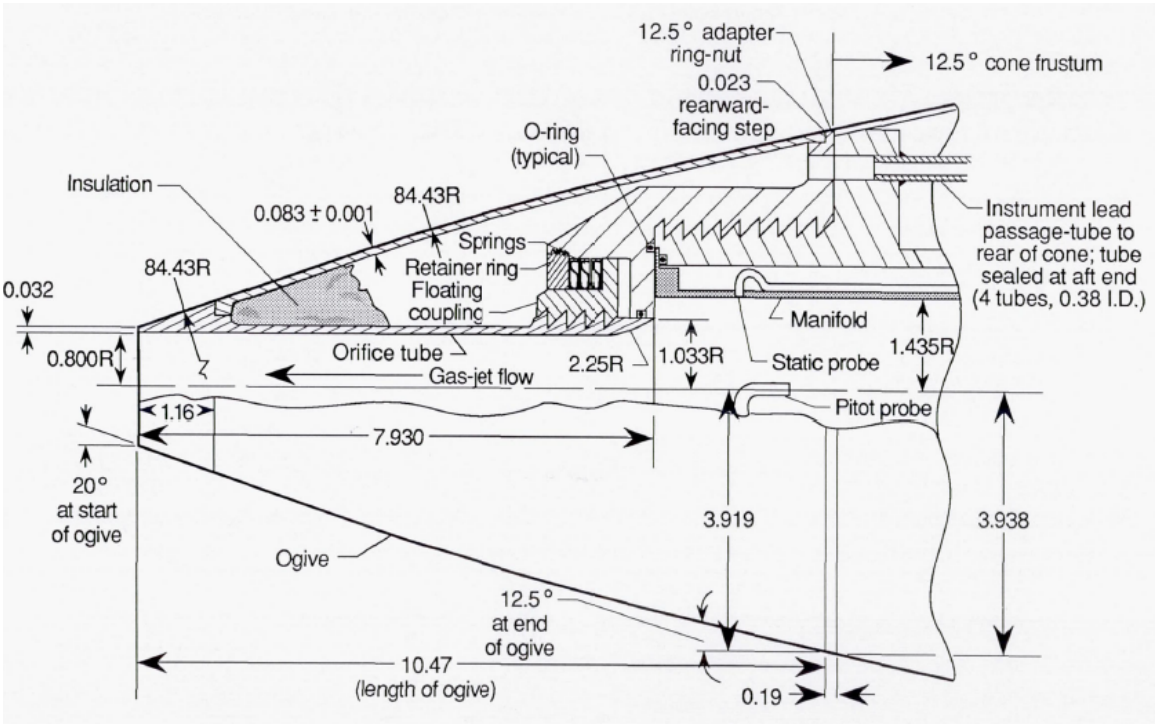


(b)

Figure 2. NASA Gasjet Wind Tunnel Model.

The conservative form of the compressible Reynolds-Averaged Navier-Stokes equations in the in-house algorithm are as follows:

$$\frac{\partial \rho}{\partial t} + \frac{\partial [\rho u_j]}{\partial x_j} = 0 \tag{2}$$

$$\frac{\partial}{\partial t}(\rho u_i) + \frac{\partial}{\partial x_j}\left[\rho u_i u_j + p\delta_{ij} - \left(1 + \frac{\mu_t}{\mu}\right)\tau_{ij}\right] = 0 \tag{3}$$

$$\frac{\partial}{\partial t}(\rho E)+\frac{\partial}{\partial x_j}\left[\rho u_j E+u_j p-\left(1+\frac{\mu_t}{\mu}\right)u_i\tau_{ij}-\left(c_p\frac{\mu}{\mathrm{Pr}}+c_p\frac{\mu_t}{\mathrm{Pr}_t}\right)\frac{\partial T}{\partial x_j}\right]=0 \tag{4}$$

Here, $\rho$ in these equations refers to the density, $p$ is the pressure, $T$ is the temperature, E is the total energy, $u$ is the velocity vector in tensor format, and the viscous stress tensor is given by:

$$\tau_{ij}=\mu\left(\frac{\partial u_i}{\partial x_j}+\frac{\partial u_j}{\partial x_i}-\frac{2}{3}\frac{\partial u_k}{\partial x_k}\delta_{ij}\right) \tag{5}$$

The numerical algorithm used to solve the Navier-Stokes equations is an implicit factorization finite center-difference scheme about a regular rectangular. Local time linearization is applied to the nonlinear terms. An approximate factorization scheme is applied to the resulting matrices, which factorizes the operator, resulting in efficient matrix equations with narrow bandwidth. This results in block tridiagonal matrices, which are easy to solve. The spatial derivatives can thus be approximated using second-order central differences. Explicit and implicit artificial dissipation terms are added to achieve nonlinear stability. A spatially variable time step is used to accelerate convergence to steady-state solutions. We selected k-ε and the Wilcox k-ω turbulence models for this investigation. Their transport equations' convection and diffusion terms are negligible in the inertial sublayer for two-equation turbulence models. Local equilibrium prevails, which implies that the production of the turbulent kinetic energy $k$ is equal to the dissipation rate. The local equilibrium condition leads to two simple relations, which can be used as boundary conditions for $k$ and the dissipation terms for incompressible and compressible flows. Further details on the computational procedures are contained in [1].

## Results and Discussion

The carbuncle problem prevailed with tenacity for the Gasjet case. As alluded to above, carbuncle instabilities have been attributed to numerical finite-difference upwind schemes, computational rounding-off errors, and instabilities in convective terms of the Navier Stokes equations. Although the steady solutions did not blow up, they remained bounded, reflecting the numerically oscillating flowfield caused by an inherent numerically-unsteady flow. The solution for the present analysis was carefully selected when the fully detached, well-formed rounded shock persisted for at least 300 iterations. The solution convergence history shown in Figure 3 confirms that the computations past the Gasjet model, particularly near the nose region, were numerically unstable.

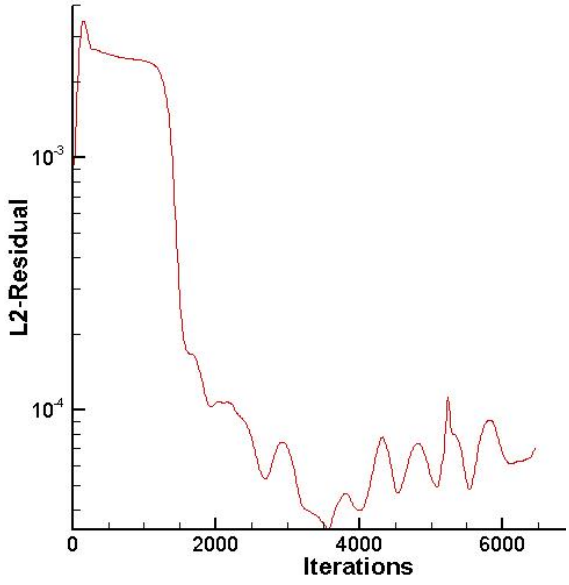

Figure 3. L2-Residual Convergence History of the Solid Gasjet Model.

Unexpectedly, a single converged solution (a fixed flow configuration) was not obtained, even with more than two orders of L2 residual convergence. However, as depicted in Figures 4a through 4c, successful solutions were obtained near the convergence regime. In Figure 4a, the flow reflecting from the flat surface at the nose is not immediately swept downstream as typically observed in the flow past round tips. Instead, it interacts very strongly against the incoming flow emerging from the leading shock, penetrating further upstream, resulting in a numerically unstable flow. The shock shape at the start of this destabilizing process is similar in appearance to the one created in a flow over a spiked nose that gradually approaches the expected rounded bow shock configuration, typical of hypersonic flow over a blunt nose. It then deforms again into a conical configuration before converging towards the bow shock shape again. The oscillations have picked this up in the residual history curve in Figure 3. This 'numerically unsteady' flow phenomenon, as discussed earlier, is most likely caused by carbuncle instability (See further Ismail and Roe [10] and Garicano-Mena et al. [11]). The occurrence of carbuncle instabilities has been attributed to numerical finite difference upwind schemes, computational rounding-off errors, and instabilities in convective terms of the Navier Stokes equations. Figures 4 show the evolutionary stages of 'unsteady' shock formation immediately upstream of the flat-surfaced Gasjet. The streamlines in Figure 4c also show reverse flow within the vicinity and downstream of the leading shock, confirming that the flow from the flat surfaces reverses and interacts with the oncoming flow from the shock.

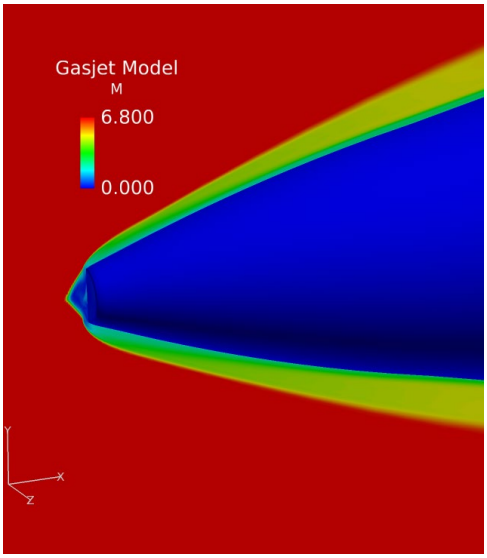


(a)

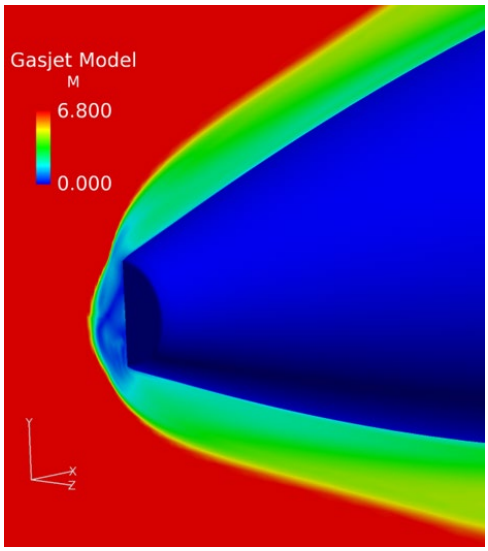


(b)

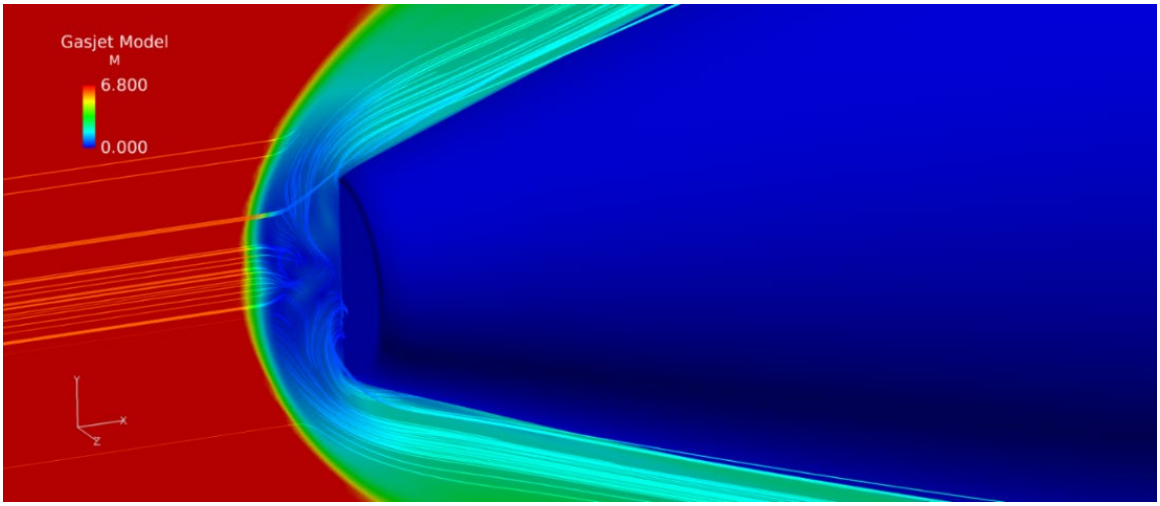


(c)

Figure 4. Solid Gasjet model during different stages towards final convergence.

As observed in the above calculations, the numerical carbuncle problem was inherently repetitive. The solution would progress towards what would appear to be a steady solution but would soon distort towards an unresolved solution characterized by the first two stages in Figure 4. It is very likely that the disturbances bouncing off the flat nose traverse upstream towards the shock and impede its evolution. Figure 5 shows the Mach- based flowfield past the 2D Gasjet model. The solution was well-behaved and converged and didn't exhibit any erratic behavior of the 3D solution. The convergence process for the 2D calculations is satisfactory, as characterized by the smooth L2 residual history shown in Figure 6, dropping more than three orders of magnitude within 3000 iterations.

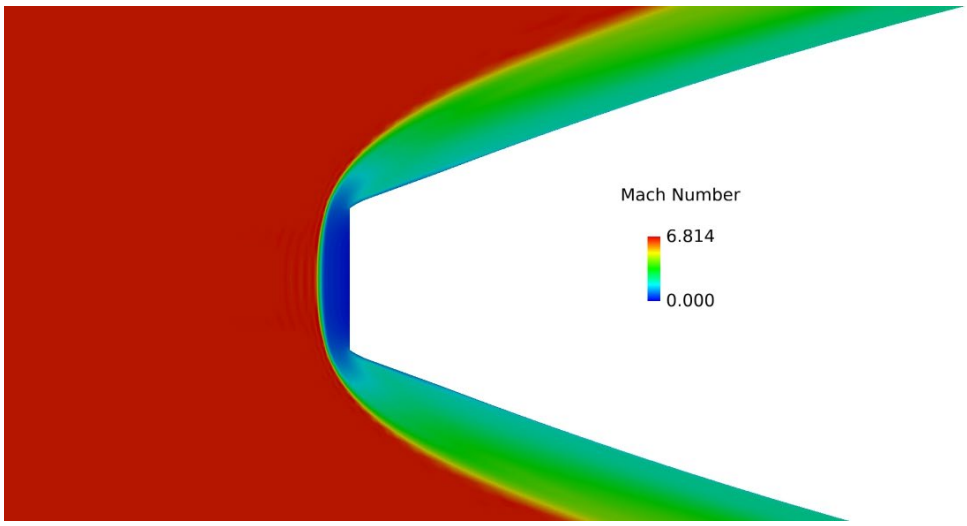


Figure 5. Mach-based flowfield past the 2D Gasjet Model.

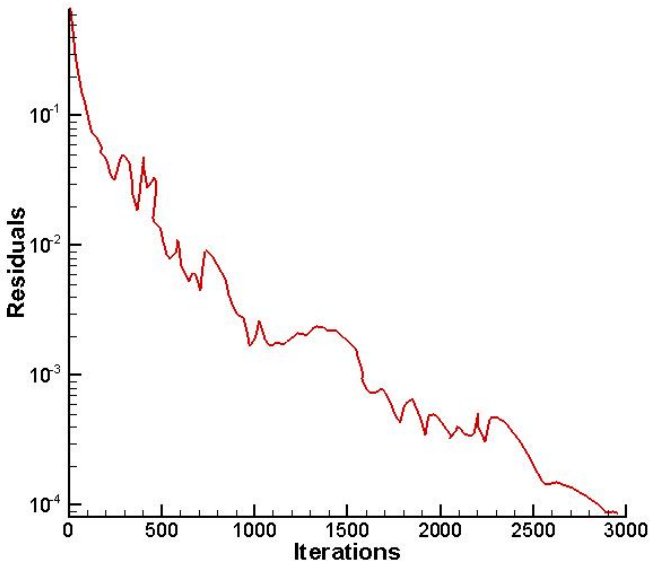


Figure 6. Convergence history of the 2D computations past the 2D Gasjet Model.

Figures 7 and 8 show the velocity contours of the 2D and 3D models, respectively, to inspect the flowfield between the shock and the flat front nose of the Gasjet model. The snapshot of the 3D model flowfield at its most converged state of the computations. It shows clearly that the flow immediately upstream of the flat nose of the 2D Gasjet model, as seen in Figure 7, is smooth, uniform, and well-behaved. No signs of unsteadiness or any other discrete disturbances are present in the flow. On the other hand, the velocities contours in the vicinity of the shock and the blunt, flat front surface contain quite chaotic flow with "pimples" of disturbance sources visible. It appears that the 3D simulation mode facilitates the formation of numerical 'clots,' around which instabilities grow and spread.

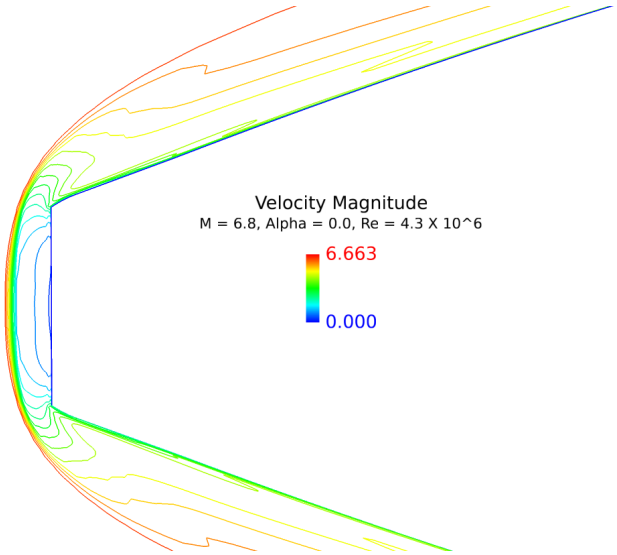


Figure 7. Flowfield past the 2D Gasjet Model.

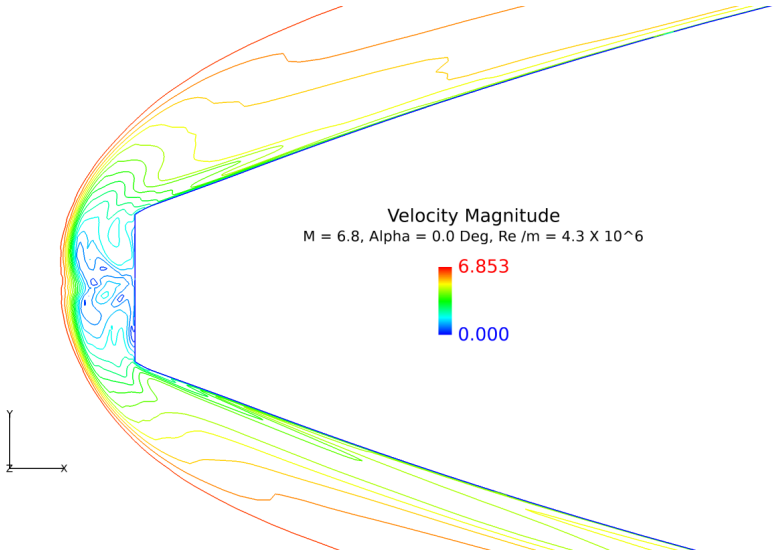


Figure 8. Flowfield past the 3D Gasjet Model.

## Conclusion

A numerical anomaly known as carbuncle was found to persist in the flowfield between the shock and the blunt, flat nose of a 3D Gasjet model. The numerical simulation fails to contend with the complexity of the flow, fraught with subsonic to hypersonic flow conditions, pressure extremes, Mach waves, and other strong entropy layer presence in this region. Various dissipation and artificial viscosity invoking schemes crafted to aid convergence may be at across purposes in this region. However, these destabilizing implications seem to subside for corresponding 2D simulations, where satisfactory and comprehensive convergence was reached without difficulty.

Although significant theoretical insight has been gained for 1D and 2D problems, no definite fixes are available to cure the carbuncle problem for complex flows in 3D. It must be understood that carbuncle is essentially a numerical simulation issue and does not exist in real flows. The present research on this carbuncle phenomenon will continue to try different numerical strategies to circumvent this problem. Since the carbuncle problem is inherently related to the erratic nature of numerical resolution near the shock axis region, a different solver scheme adapting a Penta diagonal solver in preference to the tridiagonal block matrices may be tried to formulate the equations. The Courant (CFL) number can also be varied to mitigate the numerical error accumulation. Another parameter that directly influences the numerical solution process is the variable time step which needs to be based on the local Jacobean, $\Delta t = DTCAP(1 + \sqrt{J})$, rather than the local CFL number. Some adjustment to $2^{nd}$ and $4^{th}$ order dissipation values could be attempted in conjunction with introducing an artificial viscosity in the right-hand side of the Euler portion of the equation as recommended by Kitamura [8]. It is equally possible increasing the orthogonality of the mesh in the nose region would enable the numerical simulation to 'see' the flowfield as a local 2D simulation.

## References

[1] M. Khalid and K. A. Juhany, "Innovative Means of Surface Blowing towards Heat Alleviation for Hypersonic Flows', International Journal of Aerospace Engineering, June 2019.
[2] F. Ismail, P. L. Roe and H. Nisjikawa, 'A Proposed Cure to the Carbuncle Phenomenon', Proceedings of the Fourth International Conference on Computational Fluid Dynamics, ICCFD, Ghent, Belgium, 10-14 July 2006, Springer 2009.
[3] Y. Chauvat, J. Moschetta, and J. Gressier, “Shock wave numerical structure and the carbun cle phenomenon,” *Int. J. Numer. Methods Fluids*, vol. 47, no. 819, pp. 903–909, 2005.

[4] Robinet J C, Gressier J, Casalis G, Moschetta J M (2000). Shock Wave instability and carbuncle phenomenon: same intrinsic origin? *Journal of Fluid Mechanics* 417, pp 237-263.
[5] J.-M. Moschetta, J. Gressier, J.-C. Robinet, and G. Casalis, "The carbuncle phenomenon: a genuine Euler instability?," in *Godunov Methods*, Springer, 2001, pp. 639–645.
[6] F. Kemm, "Heuristical and numerical considerations for the carbuncle phenomenon," *Appl. Math. Comput.*, vol. 320, pp. 596–613, 2018.
[7] A. V Rodionov, "Artificial viscosity to cure the carbuncle phenomenon: The three-dimensional case," *J. Comput. Phys.*, vol. 361, pp. 50–55, 2018
[8] K. Kitamura, E. Shima, and P. L. Roe, "Carbuncle phenomena and other shock anomalies in three dimensions," *AIAA J.*, vol. 50, no. 12, pp. 2655–2669, 2012.
[9] J. R. Nowak, Gasjet and tangent slot cooling film tests of a 12.5°Cone at Mach Number of 6.7, NASA Technical Paper 27866,1988.
[10] Ismail, F and P. L. Roe, 'Affordable, entropy-consistent Euler flux functions II: entropy production at shocks'. Journal of Computational Physics, 2009.
[11] Garicano-Mena J, Lani A, Deconinck H. `An energy-dissipative remedy against carbuncle: Application to hypersonic flows around blunt bodies', Computers and Fluids 2016.